

TURBOMACHINERY BLADE PROFILE DESIGN

S.Ramamurthy, Scientist, NAL, Bangalore
K.Murugesan, Scientist, NAL, Bangalore

1 INTRODUCTION

Turbomachinery blade profiles in use today were all derived out of conventional methods. For example an impulse blading of a turbine is derived out of multi circular arcs of different radii for suction surface and pressure surface with a suitable leading and trailing edge radii. The reaction bladings were designed purely out of empirism based on the amount of acceleration or Gulf factor i.e., the ratio of throat opening to pitch (Ref-1), where as compressor blade profiles were derived by imposing a suitable camber on a known base profile with a chosen thickness distribution. The performance of these profiles were assessed by conducting series of experiments which involves the measurement of surface velocity distribution and profile loss. From the experimental results each profile can be given a tag of operating range. Selection of blade profile for a given velocity distribution involves the complete scanning of experimental results, which becomes tedious and time consuming. Now a days many theoretical methods are available to evaluate the performance of the blade profile. These methods were extensively used to update the blade profiles originated during the early decades.

A theoretical method to generate turbomachinery blade profiles for a desired velocity distribution or vice versa is discussed in this paper. As an example the analysis and design of a typical turbine rotor blade profile (called conventional profile) is considered. This conventional turbine rotor blade profile was analysed theoretically for surface velocity distribution, boundary layer growth and associated profile loss. The surface velocity distribution was obtained using singularity method based on Martensen's approach (Ref-5) by assuming the flow to be two dimensional and incompressible. The boundary layer parameters were predicted using momentum integral method for laminar flow (Ref-6) and improved entrainment method for turbulent flow (Ref-7). The profile loss was estimated from the value of momentum thickness at the trailing edge and fluid outlet angle. The surface velocity distribution and profile loss were also measured experimentally in a cascade wind tunnel for comparative purposes.

The conventional profile was redesigned by reshaping the velocity distribution to get lower profile loss using the inverse Martensen's approach. The designed profile was analysed theoretically for the same fluid inlet angles for which the conventional profile was analysed earlier. Both the profiles were compared to assess their performance. This theoretical approach can be used as a design tool for generating turbomachinery blade profile for best performance.

2 NOTATIONS

- Ψ -Stream function in potential flow
- Ψ_c -Stream function due to a difference in vortex sheet
- V_a -Tangential velocity on the profile
- V_r -Required tangential velocity on the profile

nV -Imposed normal velocity on the profile due to the difference in vortex sheet
 C_{∞}, C' -Constants
 F -Green function used by Martensen
 X, Y -Coordinates of the control points on the profile
 ξ, η -Coordinates of the variable point of integration
 t -Pitch
 γ -Vortex distribution on the profile
 γ_c -Difference in vortex sheet strength
 c -Contour of the profile
 s -Distance parameter for the profile
 λ, μ -Angle parameter for the profile
 n -Unit normal to the profile
 K -Kernal function for tangential velocity
 H -Kernal function for normal velocity
 $V_{\infty x}$ -X component of main stream flow
 $V_{\infty y}$ -Y component of main stream flow
 N -Number of points on the profile
 X, Y -Coordinates of the control point after iteration
 m, n -Control point on a section of a profile
 τ_0 -Shear stress
 ρ -Density of the fluid
 θ -Momentum thickness
 δ^* -Displacement thickness
 v -Surface velocity

3 THEORETICAL METHOD

3.1 VELOCITY DISTRIBUTION

The stream function at any point (X, Y) periodic over a pitch "t" in the flow domain or on the contour is given by (Ref-2)

$$\Psi(x, y) = C_{\infty} + V_{\infty x} \cdot Y - V_{\infty y} \cdot X + \frac{1}{2\pi} \int_c F \cdot V \cdot ds$$

Where F is a Green function given by

$$F(x, y; \xi, \eta; t) = \log_e \frac{1}{\left[2 \left\{ \cosh \frac{2\pi(x-\xi)}{t} - \cos \frac{2\pi(y-\eta)}{t} \right\} \right]^{1/2}}$$

and C_{∞} is a constant.

The function F of (ξ, η) behaves close to (X, Y) like $\log(1/r)$, where "r" is the distance between the points. The velocity along a stream line is equal to the derivative of the stream function taken with respect to its normal. To satisfy the stagnation condition inside the contour it is assumed that there is a jump in velocity across the profile which becomes equal to the vortex strength on the contour. Thus the velocity and normal derivative of the stream function

has a discontinuity across the profile. This is given by

$$\left. \frac{\partial \psi}{\partial n} \right|_{\text{outside}} - \left. \frac{\partial \psi}{\partial n} \right|_{\text{contour}} = -\frac{V}{2}$$

$$\left. \frac{\partial \psi}{\partial n} \right|_{\text{contour}} - \left. \frac{\partial \psi}{\partial n} \right|_{\text{inside}} = -\frac{V}{2}$$

Taking normal derivative of the stream function on the contour and using boundary conditions (2) we get

$$V + \frac{1}{\pi} \frac{\partial}{\partial n} \int_C F \cdot v \cdot ds = 2 \left[V_{\infty x} \frac{\partial x}{\partial s} + V_{\infty y} \frac{\partial y}{\partial s} \right]$$

Introducing the parametric representation (Fig-1) $X(\lambda), Y(\lambda)$ for the contour and writing

$$V(\lambda) = \gamma(\lambda) / \left[\left(\frac{dx}{d\lambda} \right)^2 + \left(\frac{dy}{d\lambda} \right)^2 \right]$$

Equation (3) reduces to

$$\gamma(\lambda) - \frac{1}{2\pi} \int_0^{2\pi} K(\lambda, \mu; t) \cdot \gamma(\mu) \cdot d\mu = 2 \left[V_{\infty x} \frac{dx}{d\lambda} + V_{\infty y} \cdot \frac{dy}{d\lambda} \right]$$

Where γ is the vortex strength and

$$K(\lambda, \mu; t) = \frac{2\pi}{t} \left[\frac{\frac{dy}{d\lambda} \sinh \frac{2\pi [x(\lambda) - x(\mu)]}{t} - \frac{dx}{d\lambda} \sin \frac{2\pi [y(\lambda) - y(\mu)]}{t}}{\cosh \frac{2\pi [x(\lambda) - x(\mu)]}{t} - \cos \frac{2\pi [y(\lambda) - y(\mu)]}{t}} \right]$$

Taking finite number of points N on the contour section and simplifying equation (4) to algebraic summation we get

$$\gamma_m(\lambda) - \frac{1}{N} \sum_{n=1}^N K(\lambda, \mu; t) \cdot \gamma(\mu) = 2 \left[V_{\infty x} \left(\frac{dx}{d\lambda} \right)_m + V_{\infty y} \left(\frac{dy}{d\lambda} \right)_m \right]$$

This equation is set up at all the control points on the profile and solved for respective vorticities (γ). The velocity on the contour is then obtained from these vorticities.

3.2 LAMINAR BOUNDARY LAYER GROWTH

Momentum equation is given by (Ref-6)

$$\frac{\tau_0}{\rho} = V^2 \frac{d\theta}{ds} + (2\theta + \delta^*) V \frac{dV}{ds}$$

Momentum thickness and shape factor development on the profile surface is obtained by integrating and simplifying the above equation to

$$\frac{V\theta^2}{\nu} = \left(\frac{0.45}{V^5} \right) \int_0^s V^5 ds$$

$$\Lambda = \frac{\theta^2}{\nu} \cdot \frac{dV}{ds}$$

Where Λ is the shape parameter which is a function of factor and displacement thickness.

Transition from laminar to turbulent flow was assumed to occur when the local Reynolds number based on the displacement thickness becomes equal to or greater than local critical Reynolds number for stable laminar flow. Laminar flow was assumed to separate when the local value of shape factor exceeds 3.6

3.3 TURBULENT BOUNDARY LAYER GROWTH

Turbulent boundary layer was assumed to start from the point of transition. The initial value of momentum thickness for turbulent flow was made equal to that of laminar flow at the point of transition.

$$\theta_t = \theta_l$$

Initial value of shape factor for the turbulent boundary layer flow is given by

$$H_t = H_l - \Delta H$$

Where ΔH is a factor depends on Reynolds number based on the momentum thickness at the point of transition (Ref-7).

The rate at which the free stream fluid is entrained into the boundary layer is determined by the velocity defect in the outer part of the layer (Ref-8). It is given by

$$C_E = \frac{1}{V} \frac{d}{ds} [v(\delta - \delta^*)] = \frac{C_f}{2} - (H+1) \frac{\theta}{V} \frac{dv}{ds}$$

Where C_E = Non dimensional entrainment rate for non equilibrium boundary layer.

The non dimensional entrainment rate for equilibrium boundary is given by

$$(C_E)_{EQ} = 0.5 C_f \left[1 + \frac{G(H+1)}{H} \right]$$

Where $G = f(H, Re_\theta)$ and $C_f = f(H)$

The entrainment shape factor development is given by

$$\theta \frac{dH^*}{ds} = H^* (C_E)_{EQ} [F(\eta) - \eta]$$

Where $\eta = \frac{C_E}{(C_E)_{EQ}}$ and $H^* = \frac{\delta - \delta^*}{\theta}$

- $F(\eta) = 1$ for $\eta = 1$ (i.e., for equilibrium boundary layer)
- $F(\eta) = \frac{5-4\eta}{3-2\eta}$ for $\eta < 1$ (i.e., layer with Re_θ growing less rapidly than the corresponding equilibrium layer)

c) $F(\eta) = \frac{1}{2\eta-1}$ for $\eta > 1$ (i.e., for layer with Re growing less rapidly than the corresponding equilibrium layer)

3.4 PROFILE LOSS

A body placed in a stream of fluid gives rise to profile drag, which is sum of skin friction drag and pressure drag. The profile drag is directly proportional to the momentum thickness at the trailing edge. Profile drag based on momentum thickness at the trailing edge is given by (Ref-8).

$$C_{dp} = \frac{2(\theta_{tep} + \theta_{tes})}{t \cdot \sin \beta_2}$$

3.5 PROFILE SHAPE DESIGN

Both direct (Analysis) and inverse (Design) theoretical methods will be used iteratively for the blade profile design. A desired velocity distribution along the contour will be specified from the forward stagnation point to the trailing edge in terms of arc length measured along the profile from the forward stagnation point on both suction and pressure surfaces. For a conventional profile or for the profile to be modified, the velocity distribution was obtained by solving the direct problem for specified stagger and inlet conditions. The resultant velocities round the blade contour are then compared with the values of desired velocities and a set of velocity differences are computed at the control points. The vortex strengths equal to these differences in velocities will be imposed on the contour at the respective control points. These vortex strengths will give rise to normal velocities on the contour. These normal velocities violates streamline to follow the profile contour. Then the new slope of the profile at each of the control point is changed by a value equal to the ratio of normal velocity to the total imposed tangential velocity. Integration of the new slope of the contour gives new profile. Thus obtained new profile is then subjected to second direct analysis and resulting velocity distribution was compared with the desired velocity distribution and the process is repeated until convergence is obtained.

Martensen stream function equation is given by

$$\psi_c = C' + \frac{1}{2\pi} \int_c F \cdot \gamma_c(s) \cdot ds$$

Where ψ_c is the stream function for the difference in vortex sheet from the velocity differences as

$$\gamma_c(s) = V_h(s) - V_a(s)$$

The first term on the right being the desired velocity and the second the result of direct analysis. The normal velocity is obtained by taking the derivative of equation (11) w.r.t the distance "s" or preferably w.r.t the parameter

Differentiating equation (11) w.r.t λ we get

$$nV(\lambda) = \frac{1}{2\pi} \int_0^{2\pi} H(\lambda, \mu; t) \cdot Y_c(\mu) \cdot d\mu$$

Where μ denote the variable under integration.

$$H(\lambda, \mu; t) = \frac{\pi}{t} \left[\frac{\frac{dx}{d\lambda} \sinh 2\pi \left[\frac{x(\lambda) - x(\mu)}{t} \right] + \frac{dY}{d\lambda} \sin 2\pi \left[\frac{Y(\lambda) - Y(\mu)}{t} \right]}{\cosh 2\pi \left[\frac{x(\lambda) - x(\mu)}{t} \right] - \cos 2\pi \left[\frac{Y(\lambda) - Y(\mu)}{t} \right]} \right]$$

The integral in equation (13) is approximated by algebraic summation

$$nV_m = \frac{1}{N} \sum_{n=1}^N H_{mn} \cdot Y_n$$

The contour which now has a known normal velocity distribution nV across it and a tangential velocity equal to the desired value V_r must have a local slope given by

$$\frac{dn}{ds} = \frac{nV}{V_r}$$

The slope of the new contour can be obtained from the original one by a suitable integration of this change in slope. The new contour may be considered to be made up of the same elements of lengths as the previous one, but each segment will have a slope which differs by the above amount from its previous value. Thus the X-coordinates of the new contour of the two successive points (i-1) and i will be related to the X-coordinates of the same points of the old contour by the relation

$$(X'_i - X'_{i-1}) = (X_i - X_{i-1}) - \left(\frac{S_i - S_{i-1}}{2} \right) \left[\left(\frac{dn}{ds} \right)_i + \left(\frac{dn}{ds} \right)_{i-1} \right] \left(\frac{dY}{ds} \right)_i$$

or preferably in terms of λ parameter

$$(X'_i - X'_{i-1}) = (X_i - X_{i-1}) - \frac{1}{2} \left[\left(\frac{dn}{ds} \right)_i + \left(\frac{dn}{ds} \right)_{i-1} \right] \left(\frac{dY}{d\lambda} \right)_i d\lambda$$

Similarly the Y-coordinates of the new contour will be related to the Y-coordinate of the previous one by

$$(Y'_i - Y'_{i-1}) = (Y_i - Y_{i-1}) + \frac{1}{2} \left[\left(\frac{dn}{ds} \right)_i + \left(\frac{dn}{ds} \right)_{i-1} \right] \left(\frac{dX}{d\lambda} \right)_i d\lambda$$

By adding up the changes of co-ordinates for all the points from i=1 to i=m, it follows that

$$(X'_m - X'_1) = (X_m - X_1) - \frac{1}{2} \sum_{i=2}^m \left[\left(\frac{dn}{ds} \right)_i + \left(\frac{dn}{ds} \right)_{i-1} \right] \left(\frac{dY}{d\lambda} \right)_i d\lambda$$

$$(Y_m' - Y_1') = (Y_m - Y_1) + \frac{1}{2} \sum_{i=2}^m \left[\left(\frac{dn}{ds} \right)_i + \left(\frac{dn}{ds} \right)_{i-1} \right] \left(\frac{dx}{d\lambda} \right)_i d\lambda$$

If X_1', Y_1' and X_1, Y_1 are assumed to be the same point, then the position and shape of the new contour will be completely obtained.

4 RESULTS AND DISCUSSIONS

A turbine rotor blade profile (Fig-2) chosen for the initial analysis was derived out of multicircular arc with large leading edge radius. This profile was analysed theoretically for surface velocity distribution for a given stagger, pitch to chord ratio, inlet velocity, fluid inlet angle.

The surface velocity normalised w.r.t outlet velocity was plotted against non-dimensional surface distance. The surface velocity distribution (Fig-3) at an inlet angle of 22 Degrees (Zero incidence) indicates it is a typical characteristics of a multi circular arc profile. The flow on the suction surface accelerates at a constant rate from the stagnation point upto ten percent of the surface distance. Around this point the acceleration rate suddenly decreases and the flow accelerates at a slower rate. Further downstream the surface velocity remains more or less constant followed by a sudden deceleration. On the pressure surface the flow continuously accelerate from the leading edge upto trailing edge.

The surface velocity distribution for this profile was measured in a cascade tunnel for an outlet Mach number = 0.4 and for the same fluid inlet angle, pitch/chord ratio. The measured surface velocity distribution agrees close to the theoretical velocity distribution (Fig-3) except in the regions where the local Mach numbers are quite high.

The predicted boundary layer growth for the analysed velocity distribution is shown in Figure-4. The associated profile loss is indicated in the same figure. The flow is initially assumed as laminar starting from the stagnation point with zero momentum thickness. Laminar flow becomes turbulent on both the surfaces. A sharp increase in shape factor after transition point is due to sudden deceleration. It is also observed that the boundary layer growth on the suction surface is much larger than on the pressure surface.

The velocity distribution was reshaped from the consideration of boundary layer growth and profile loss. For this reshaped velocity distribution a new profile was designed. The velocity distribution on the suction surface of the initial conventional profile shows discontinuities and a steep adverse pressure gradient around mid chord position. This was reshaped into a new desired velocity distribution with gradual change in slope and a more moderate and distributed rate of deceleration over the suction surface starting from about 30% of chord (Fig-5). The profile shape obtained after third iteration is shown in Figure-6. In the same figure the conventional profile is also shown. The outlet flow angle and blade loading of the designed profile agrees close to the conventional profile.

The designed profile was analysed theoretically for

Reprint from Proceedings of

3rd National Conference on Aerodynamics,
27-28 November 1987, IIT, Bombay.

surface velocity distribution at same inlet conditions for which conventional profile was analysed. The surface velocity distribution obtained is shown in Figure-6. The sudden flow deceleration noticed in the velocity distribution of an conventional profile is not seen in the velocity distribution of the designed profile. The flow continuously accelerates from the leading edge to the trailing edge on the pressure surface where as on the suction surface the velocity remains more or less constant except for an initial acceleration near the leading edge.

The boundary layer analysis was carried out for this designed profile for ideal outlet Mach number = 0.4. The predicted shape factor and non-dimensional momentum thickness values for various non-dimensional surface distance are shown in Figure-7. The associated profile loss is also indicated in the same figure. The flow on the pressure surface is fully laminar. On the suction surface the transition point moves towards leading edge with larger region of turbulent flow. The rate of increase in shape factor immediately after transition point is reduced. The boundary layer growth and hence the associated profile loss value are smaller than that of the conventional profile.

The predicted outlet conditions for the designed and conventional rotor blade profile for the inlet angles considered are tabulated in Table-I for comparative purposes. The designed and conventional profiles were theoretically analysed for two extreme incidence angles to assess their performance. The estimated profile loss for both the profiles at these incidence angles are given in Table-II. It is observed from this table about twenty percent reduction in profile loss was achieved for the designed profile as compared to the conventional profile. We see from Table-I, the lift coefficient for both the profiles were approximately same. This is necessary to keep the work done per stage same. The profile was optimised by minimising the drag coefficient (i.e., profile loss) for the same lift coefficient. Hence maximising C_L/C_D .

5 CONCLUSIONS

The surface velocity distribution of the conventional blade profile indicates that it is a typical characteristics of a profile derived out of multi circular arc. The boundary layer analysis showed that the turbulent flow on the pressure surface had a tendency to separate after the point of transition. The boundary layer growth and associated profile loss coefficients are quite high. The velocity distribution indicated its reshaping for optimum profile.

For the same inlet and outlet flow conditions the surface velocity distribution obtained for the designed profile was better than the conventional profile. The boundary layer analysis showed that the boundary layer growth is smaller and the tendency of turbulent flow separation on the pressure surface of the profile was avoided. Considerable reduction in profile loss was achieved for this profile. Both from the consideration of surface velocity distribution and boundary layer growth the new profile is superior than the conventional profile.

This design method controls directly the performance of the blade. The method can be used as a powerful design tool for generating

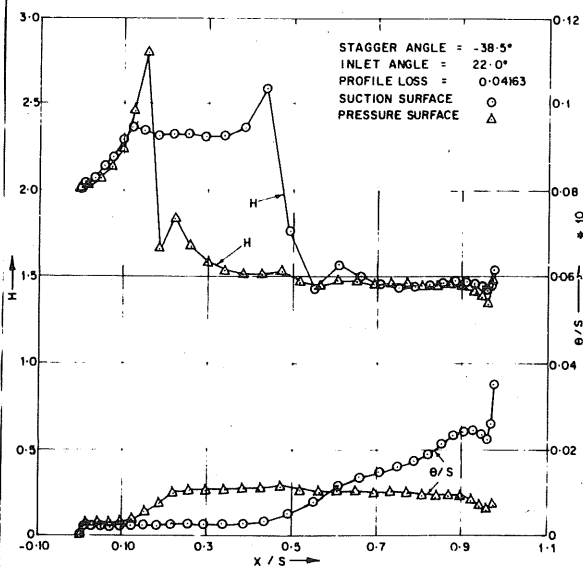
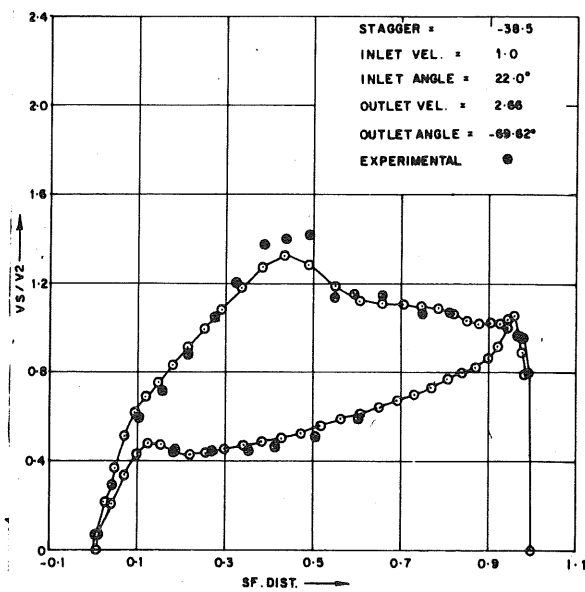
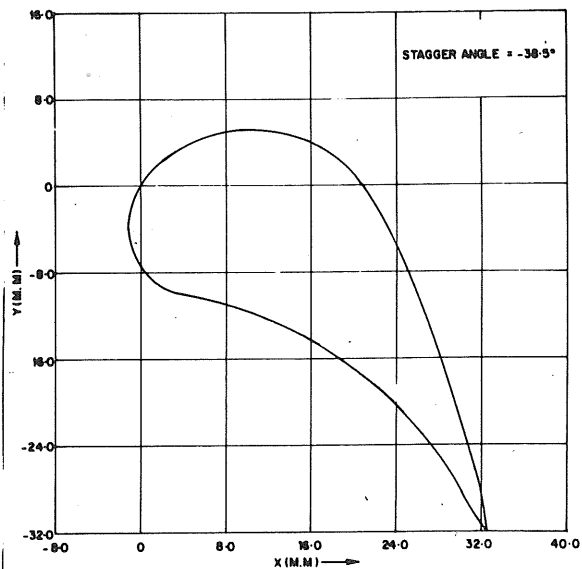
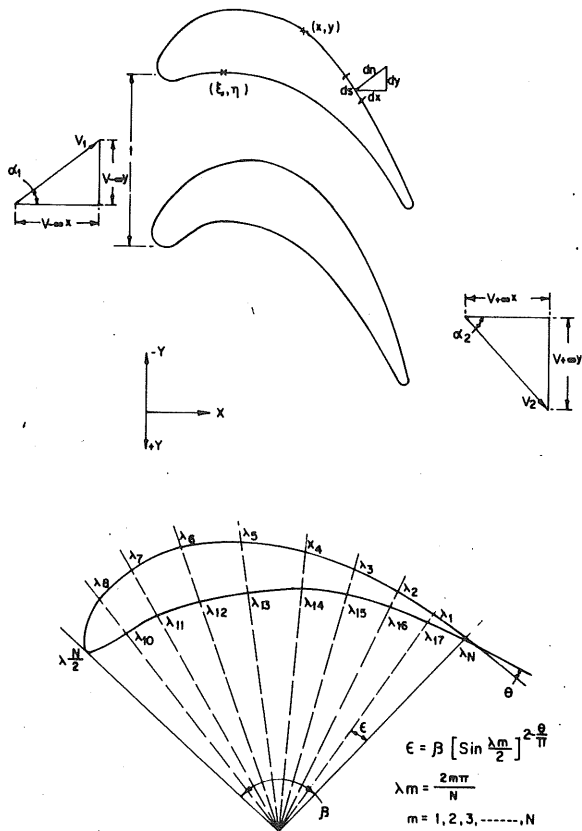
new blade profiles or modifying the existing blade profiles for optimum stage performance.

6 ACKNOWLEDGEMENTS

Mr.R.Rajendran, JTA of Propulsion Division, N.A.L. helped the authors in preparing this manuscript. The help given by him is sincerely acknowledged.

7 REFERENCES

1. Shephred, D.G. - Principles of Turbomachinery, The Macmillan Company.
2. Martensen, E. - Berechnung der Druckverteilung an Gitterprofilen mit einer Fredholmschen Integralgleichung
Archive for rotational mechanics and analysis.
Vol. 3, No. 3, 1959 ,pp:235-270
3. Murugesan, K. - Numerical Solution of Ideal Flow Through Tandem
Railly, J.W. Cascades, Research Report No. 101
Dept. of Mech. Engg., University of Birmingham, 1969.
4. Thwaites, B. - Incompressible aerodynamics, Oxford Press 1960.
5. Schlichting, H. - Boundary Layer Theory
6. Head, M.R. - Improved Entrainment Method For Calculating
Patel, V.C. Turbulent Boundary Layer Development.
ARC R&M No. 3643, 1970
7. Murugesan, K. - Two Dimensional Design Of Multi Sectional
Railly, J.W. Profiles Isolated or in Cascades.
8. Schlichting, H. - Application of Boundary Layer Theory in
Turbomachinery. Jl. of Basic Engg.
Trans. of the ASME Dec-1955, PP:543-551



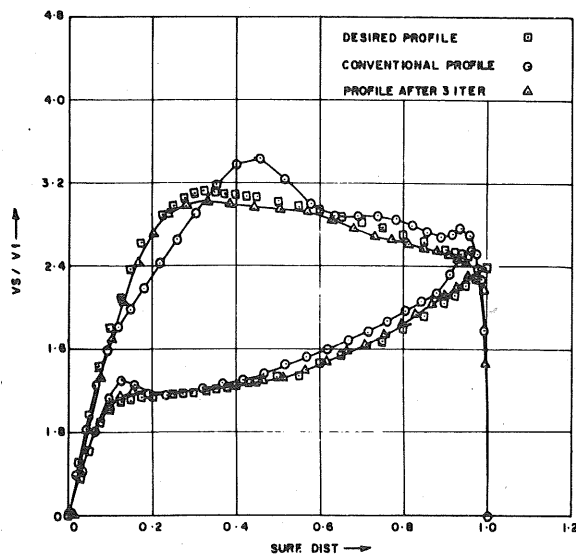


FIG. 5 VELOCITY DISTRIBUTION (CC-MM)

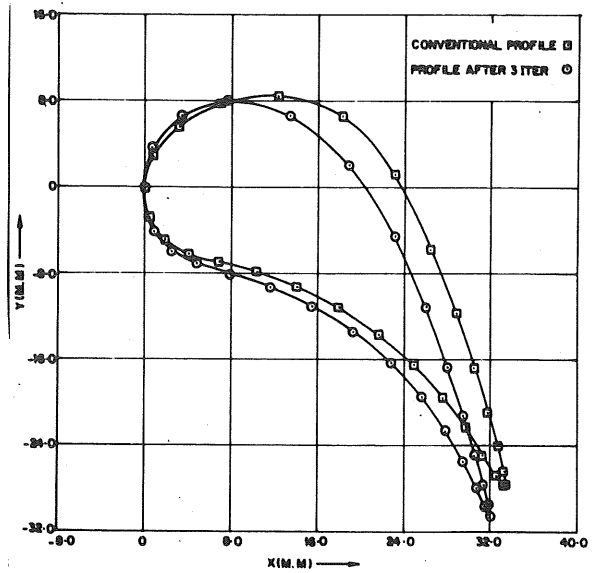


FIG. 6 DESIGNED AND CONVENTIONAL PROOF. (CC-MM)

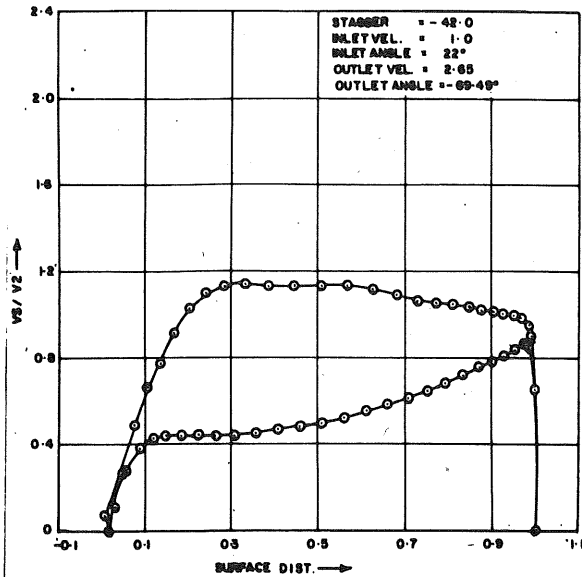


FIG. 7 VELOCITY DISTRIBUTION (DESIGNED PROFILE)

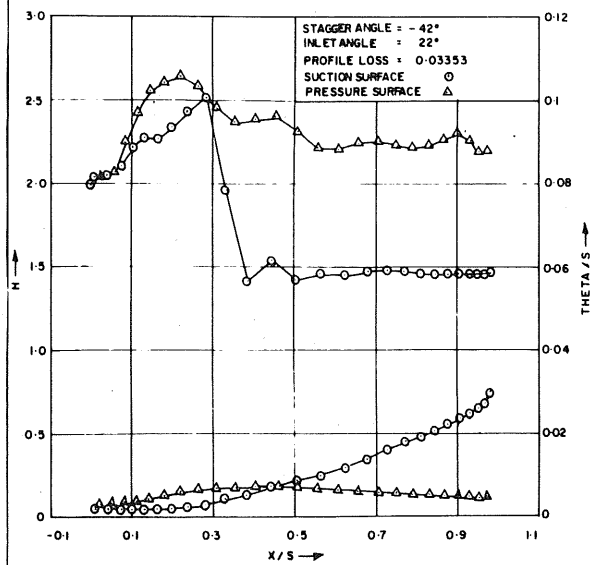


FIG. 8 B. L. GROWTH (DESIGNED PROFILE)

Table-I

Comparison Between Conventional and Designed Profile

Inlet Angle (deg)	22°		52°		-8.0°	
	CP	DP	CP	DP	CP	DP
Incidence (deg)	0.0	18.0	30.0	40.0	-30.0	-20.0
V_2/V_1	2.66	2.65	1.77	1.76	2.84	2.83
Outlet Angle (deg)	69.62	69.49	69.61	69.47	69.63	69.49
Lift Coefficient	6.41	6.16	2.97	2.91	6.92	6.59

Table-II

Profile Loss Coefficient Comparison

Inlet Angle	22.0°	52.0°	-8.0°
C_{DCP}	0.04163	0.05002	0.04160
C_{DEX}	0.0380	0.0510	0.0375
C_{DP}	0.0335	0.04008	0.0317
$\Delta C_p\%$	19.5	19.9	23.8